Wide-Dynamic-Range "Neutron Bang Time" Detector on OMEGA

Introduction

Measurements of the neutron emission from inertial confinement fusion[1] (ICF) implosions provide important information on the target performance, which can be compared directly with numerical models. Targets filled with deuterium (D_2) or a deuterium–tritium (DT) mixture are heated either by direct laser illumination or by soft x-ray radiation in a laser-heated hohlraum. In the resulting implosion, the target is compressed to conditions under which thermonuclear fusion occurs. Fuel atoms undergoing fusion release energetic charged particles, photons, and neutrons. The time of peak neutron emission—the "neutron bang time"—is very sensitive to the details of the energy absorption and the hydrodynamic response of the target. Several detectors that measure the neutron bang time[2–4] have been described in the literature. These include a fast (<25 ps) streak camera–based neutron temporal diagnostic[5] (NTD), which is also capable of resolving the details of the neutron burn history. The NTD is currently installed on LLE's OMEGA laser. It needs a minimum neutron yield $>10^9$ to measure the bang time and is incompatible with D_2 cryogenic target experiments due to mechanical constraints. These drawbacks, plus the complexity and cost of streak camera–based measurements, motivated the development of an alternative neutron bang time detector. This article describes a simple, low-cost, wide-dynamic-range, neutron bang time (NBT) detector that has been developed to complement the capabilities of the NTD.

Setup of the Detector System

The NBT is shown schematically in Fig. 88.1. It is composed of two detector channels to increase the dynamic range of the instrument, an optical fiducial system to cross-time the

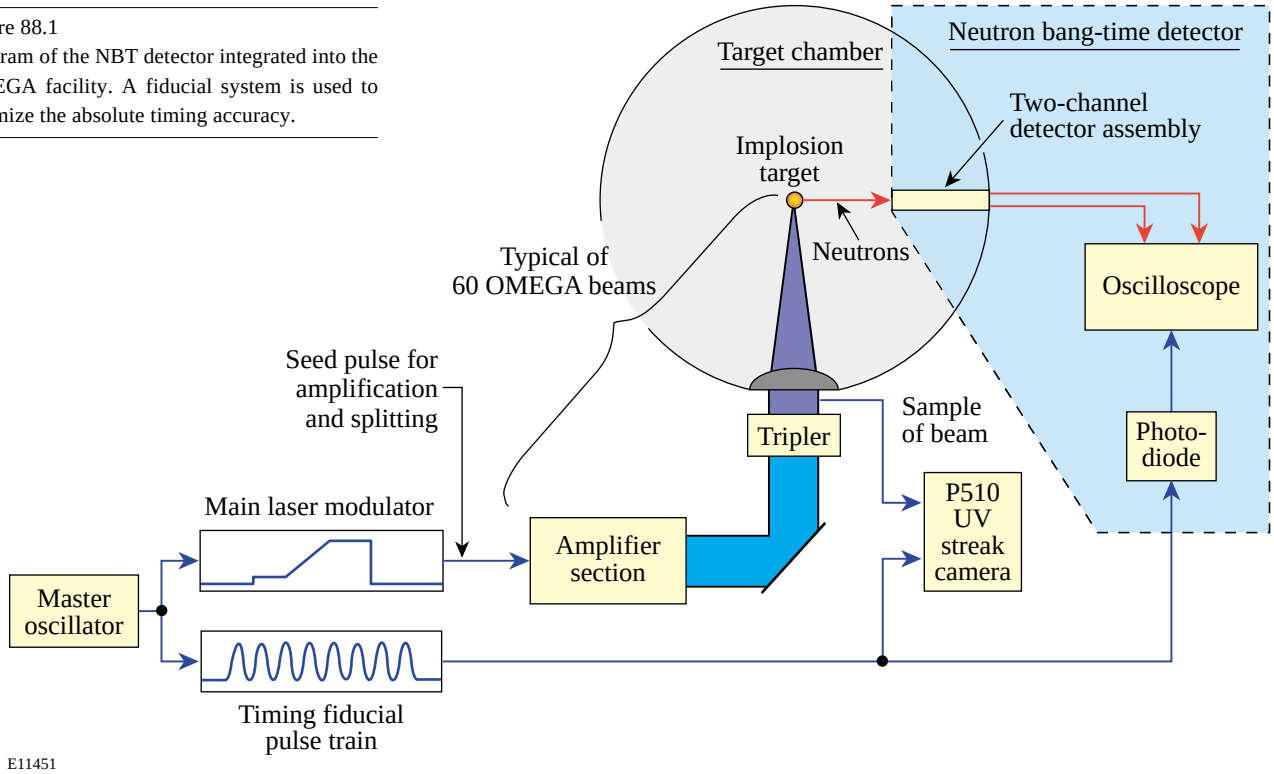

Figure 88.1
Diagram of the NBT detector integrated into the OMEGA facility. A fiducial system is used to optimize the absolute timing accuracy.

diagnostic to the laser pulse, and a fast digitizing oscilloscope. As shown in Fig. 88.2(a), each channel of the NBT system consists of a fast, quenched plastic scintillator (Bicron BC-422Q[6]) coupled to a photomultiplier tube (PMT; Hamamatsu H5783[7]). The H5783 PMT uses an integrated high-voltage power supply that requires only a 15-V dc input. This voltage is supplied through the signal cable using two high-bandwidth bias tees[8] to avoid ground loops and electromagnetic interference (EMI) noise pickup on the dc feed. The gain of the PMT is set by a voltage divider based on a reference voltage supplied by the H5783 to optimize the signal-to-noise ratio of the detection system. Both channels are packaged into a lead housing with copper foil wrapping to provide x-ray and EMI shielding. The efficient x-ray shielding and EMI shielding makes it possible to use the NBT as a secondary neutron or hard x-ray detector in an energy range above 500 keV.[9]

As is shown in Fig. 88.2(b), the NBT detector assembly is positioned approximately 55 cm from the target chamber center (TCC) in a 3.8-cm-diam reentrant tube. Due to the small diameter of the reentrant tube, the second channel is located behind the first along the flight path of the neutrons produced in the target. This does not reduce the sensitivity of the back channel because of the long mean free path of the energetic neutrons in matter. To maximize the dynamic range of the system, different-sized scintillator volumes were selected for

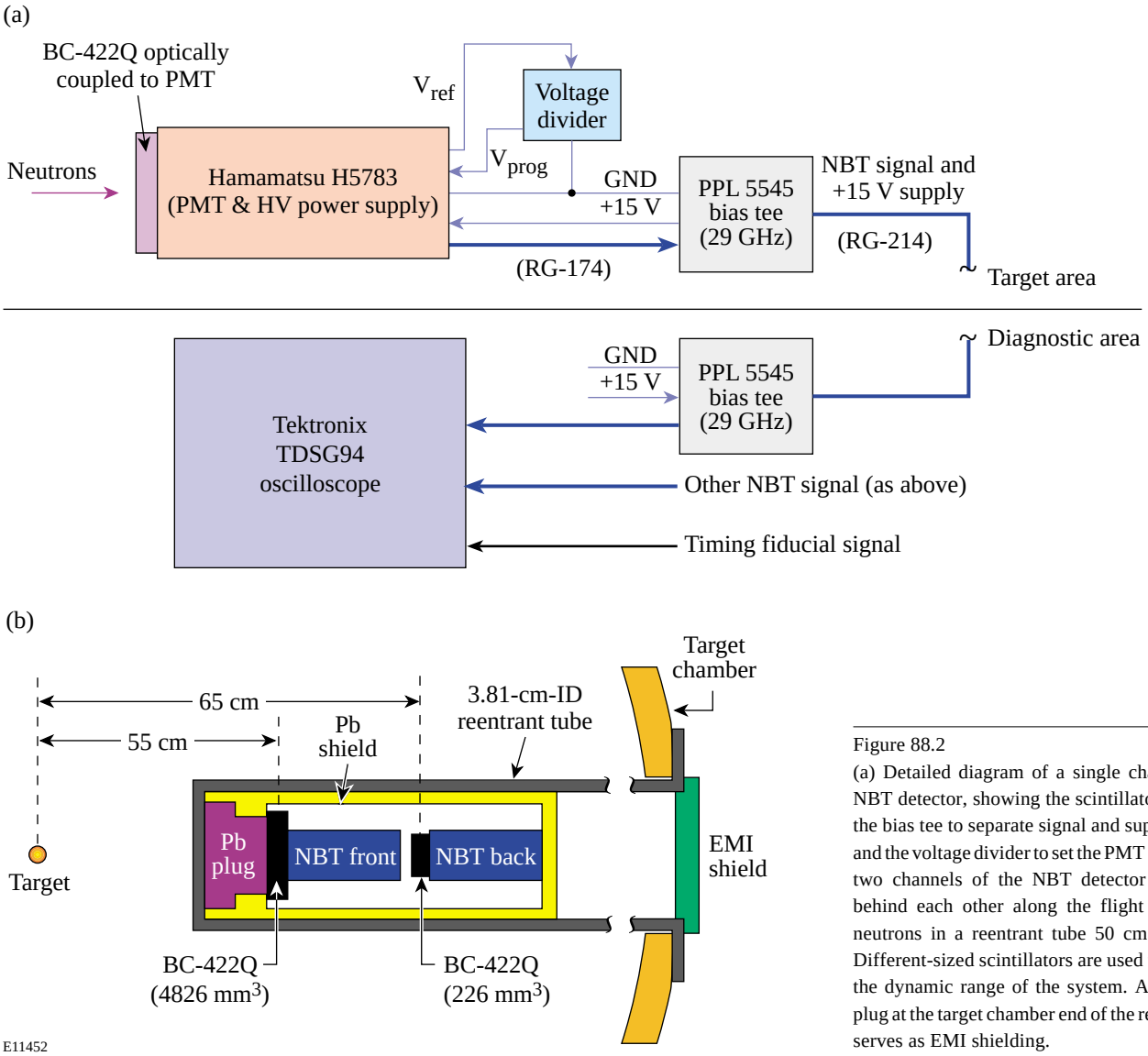

Figure 88.2
(a) Detailed diagram of a single channel of the NBT detector, showing the scintillator, the PMT, the bias tee to separate signal and supply voltage, and the voltage divider to set the PMT gain. (b) The two channels of the NBT detector are located behind each other along the flight path of the neutrons in a reentrant tube 50 cm from TCC. Different-sized scintillators are used to maximize the dynamic range of the system. An aluminum plug at the target chamber end of the reentrant tube serves as EMI shielding.

each NBT channel, 4820 mm^3 for the front channel and 230 mm^3 for the back channel. The signals from the two NBT channels are recorded on separate channels using a four-channel Tektronix TDS694,[10] 3-GHz digital oscilloscope at a sampling rate of 10 GS/s.

Absolute timing of the neutron bang time to better than 100 ps is accomplished using the OMEGA optical fiducial system. The fiducial pulse train consists of eight peaks spaced 548 ps apart and is synchronized to the shaped OMEGA laser pulse with a jitter of less than 20 ps. The optical fiducial is amplified separately from the main laser pulse and delivered to numerous system diagnostics. The fiducial pulse train is recorded on a separate channel of the NBT oscilloscope using a fast photodiode and also on the P510 ultraviolet streak camera,[11] which measures the laser pulse shape. The common optical fiducial serves as a reference for both the neutron signal and the laser pulse, enabling very accurate timing of the NBT signals.

Characterization of the NBT Components

The impulse response of the PMT was measured using a 100-fs laser pulse at 400-nm wavelength recorded on a 1-GHz sampling scope and found to be $\tau_{rise} = 940$ ps. Using the well-known relation

$$\tau_{rise}^{PMT} = \sqrt{\tau_{rise}^2 + \tau_{scope}^2}$$

with $\tau_{scope} = 350$ ps[10] describing the rise time of the scope, the rise time of the PMT is found to be $\tau_{rise}^{PMT} = 650$ ps, in excellent agreement with the value given by the manufacturer.[7]

A low-jitter timing reference signal is critical to accurate measurement of the neutron bang time because the electrical oscilloscope trigger signal has a jitter relative to the laser pulse in excess of 100 ps. The simple solution of routing an optical fiducial fiber into the NBT detector and optically adding the fiducial pulse train to the scintillator signal does not provide a high-quality fiducial signal at the oscilloscope because the rise time of the PMT is slower than the fiducial peak spacing of 548 ps. Recording the optical fiducial pulse train using a high-bandwidth photodiode on a dedicated oscilloscope channel provides a high-quality fiducial signal where every fiducial peak is clearly resolved. The use of a separate channel for the fiducial does not degrade the timing accuracy significantly because the jitter between two channels of the TDS694 is reported by the manufacturer to be less than 10 ps. Sub-pixel resolution of the fiducial timing is accomplished by fitting a pulse train of eight Gaussian pulses spaced at the well-characterized period of $d_t = 548$ ps:

$$\text{fidu}(t) = \sum_{i=0}^{7} a_i \exp\left\{-\left[t - (t_0 + i \times dt)\right]^2 / 2\sigma\right\}$$

to the recorded signal. Here a_i is the amplitude of each fiducial peak, t_0 is the time of the first fiducial pulse, and σ is the width of an individual fiducial pulse. An example of the fiducial signal together with the fitted Gaussian pulse train is presented in Fig. 88.3 showing very good agreement between signal and fit.

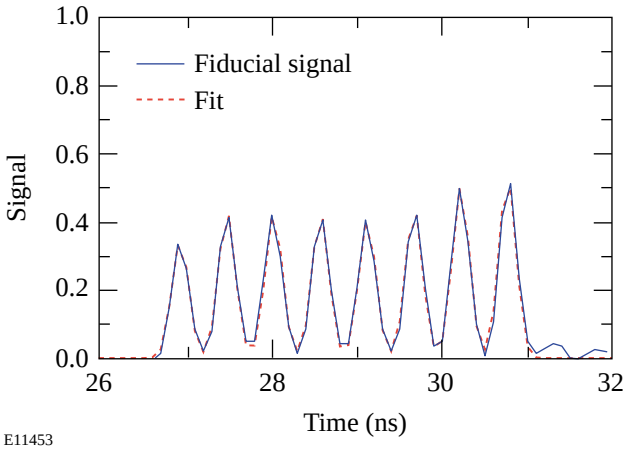

Figure 88.3
Optical fiducial and corresponding fit as recorded on the TDS694 oscilloscope. The high bandwidth of the oscilloscope makes it possible to see each individual fiducial pulse and to get a high-quality fit to obtain sub-pixel time resolution.

Because the output voltage of the PMT is limited to 5 to 10 V, EMI noise pickup effectively limits the dynamic range of each NBT detector channel. Several different shielding layers are used to limit the EMI noise to an acceptable level. The PMT is electrically isolated from the target chamber using the signal cable as its ground connection to the oscilloscope. The use of bias tees avoids ground loops in the dc power feed for the integrated PMT/high-voltage power supply. The lead housing was covered with a layer of Cu foil and grounded to the target chamber. The feedthrough holes for the signal cables were made as small as possible to limit high-frequency EMI penetration of the NBT housing. Finally, to improve the shielding, the reentrant tube was covered with an aluminum plug with only two small openings for the two signal cables. This

combined EMI shielding reduces the pickup noise from several 100 mV down to less than 10 mV for the front channel and less than 40 mV for the back channel.

The recorded neutron signal is broadened by several different mechanisms. Because the neutrons are produced at a high temperature, thermal broadening leads to a Gaussian shape of the arrival times. The plastic scintillator has a very short rise time followed by a relatively slow exponential decay.[6] Scattering processes in the housing and lead shielding also create a tail in the neutron signal that has an effect similar to the scintillator decay. The effect of the finite neutron transit time through the scintillator[12] is less important for determining the bang time than it is for measuring the neutron-averaged ion temperature and can be approximated by a Gaussian for simplicity. The electronic part of the instrument response, which can be described also by a Gaussian, results from the finite bandwidth of the photomultiplier tube, the cable, and the oscilloscope.

Overall, the measured signal $m(t)$ can be approximated by a convolution of a Gaussian $g(t)$ and an exponential decay $d(t)$, as described in detail in Ref. 12:

$$g(t) = \frac{A}{\sqrt{2\sigma}} \exp\left[-\frac{(t-t_1)}{2\sigma}\right],$$

$$d(t) = \frac{1}{\tau} \exp\left(\frac{-t}{\tau}\right),$$

$$m(t) = g(t) \otimes d(t),$$

$$m(t) = \frac{A}{2\tau} \exp\left[-\frac{(t-t_1)}{\tau}\right]$$

$$\times \exp\left(\frac{\sigma^2}{2}\right)\left\{1 + \operatorname{erf}\left[\frac{(t-t_1)-\sigma^2/\tau}{\sqrt{2\sigma^2}}\right]\right\}.$$

This function is fitted to the measured signal to improve the accuracy of the bang-time determination, especially in situations of low signal-to-noise ratio (see Fig. 88.4). Because the decay time of the scintillator and the neutron scattering effects are identical for every shot, a best-fit decay time can be determined once and used to analyze all of the data. The value used for this setup is $\tau = 1.5$ ns for both the front and the back channels. The signal amplitude A, arrival time t, and signal width σ change from shot to shot and are fitted for every measurement to optimize timing accuracy.

Figure 88.5 shows the dynamic range in D_2 neutron yield for the current two-channel NBT setup. To show more clearly the limits of the linear PMT response, the NBT signal is shown in amplitude rather than collected charge (which would be more appropriate for a neutron-yield detector). In collected

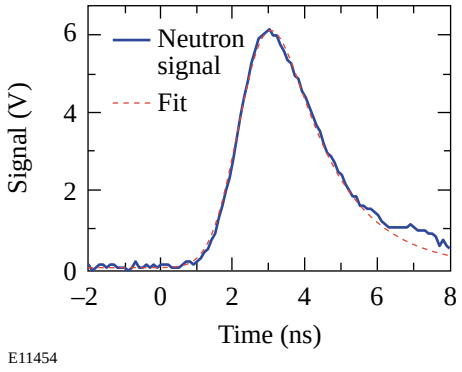

Figure 88.4
Neutron signal and corresponding fit on one channel of the NBT detector.

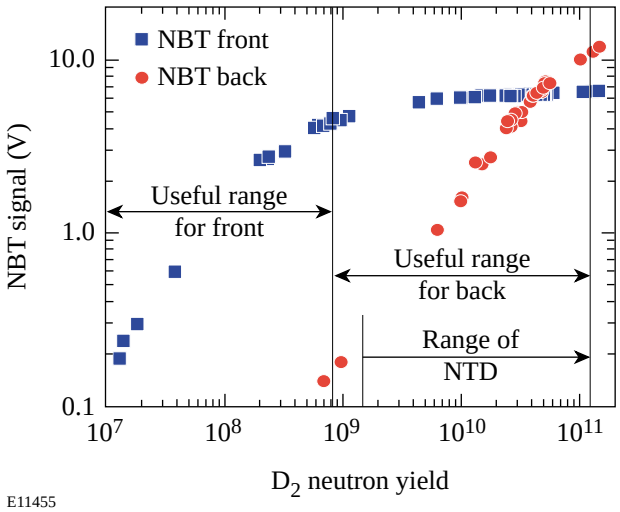

Figure 88.5
Demonstrated dynamic range of the two-channel NBT detector setup. The detection threshold for the front channel is set by the yield that results in a single neutron hit. The threshold for the back channel is determined by the EMI noise pickup.

charge, the PMT's show an even larger dynamic range that eventually distorts the temporal pulse shape. This makes it very difficult to determine the pulse arrival time and introduces large errors. The dynamic range for DT neutrons is very similar to the D_2 neutron dynamic range because, while the higher neutron energy results in a higher average signal per interacting neutron, the effect is mostly offset by the lower interaction cross section.

The front channel is relatively immune to EMI noise because even a single neutron hit results in a signal of the order of 100 mV due to the high PMT gain in the front channel. The EMI pickup noise affects mostly the back channel. A useful dynamic range from about 1×10^7 to 1×10^{11} can be realized in the present two-channel configuration.

Temporal Calibration and Bang Time Accuracy

The front NBT channel can be temporally calibrated using the hard x-ray emission from a Au target irradiated with a short (100 ps) laser pulse at best focus. To obtain a measurable signal for this calibration, the lead shield in front of the detector is replaced by a lead shield with a small hole. Previous experiments using the NTD have shown that the x-ray pulse closely follows the temporal shape of the laser irradiation.[5] Figure 88.6 shows an x-ray-induced signal recorded by the front-channel NBT, a curve fit to this signal using the expression described in the previous section, and the shape of the 100-ps laser pulse as recorded on the OMEGA UV streak camera system.[11] The effects of the limited bandwidth and the noise on the recorded signal are clearly seen, but the accuracy of determining the signal peak is improved considerably by the fitting procedure. The discrepancy that is apparent between the signal and the fit at the end of the pulse is attributed to the use of the expression that was derived for neutrons. Scattered x rays do not change speed as neutrons do, so the tail-off that is characteristic of the neutron signal is not present on the x-ray signal. This effect contributes approximately σ_{calib} = 50 ps uncertainty to the calibration.

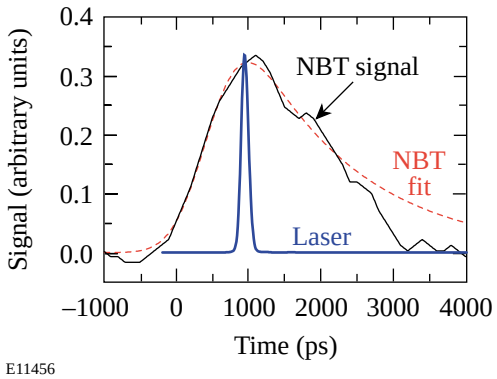

Figure 88.6
Front-channel NBT signal and corresponding fit for a hard x-ray emission produced by a 100-ps laser pulse irradiating a gold target at best focus. The 100-ps laser pulse is shown for comparison.

The x-ray calibration can be easily carried over to the neutron measurements using the propagation delay difference from the TCC to the scintillator between x rays and neutrons:

$$\Delta t_n = L_{\text{scint}}\left(\frac{1}{v_n} - \frac{1}{c}\right),$$

where $v_n^{D_2} = 2.16$ cm/ns and $v_n^{DT} = 5.12$ cm/ns are the neutron velocities and L_{scint} = 55 cm (the distance between TCC and the scintillator). A measurement uncertainty in the scintillator distance of the order of 1 mm is estimated. This corresponds to a calibration error of $\sigma_{\text{dist}}^{D_2} = 50$ ps for D_2 and $\sigma_{\text{dist}}^{D_2} = 20$ ps for DT neutrons. The scintillator distance can be measured *in situ* using the arrival-time difference between DT and D_2 neutrons for implosions of nominally identical bang time and was found to agree within the measurement error of the geometric measurement.

The back channel cannot be calibrated using this x-ray technique because the PMT and bias tee of the front channel effectively shield the back-channel detector from the hard x rays produced by the timing target. This channel can be cross calibrated to either the front channel in the common range of sensitivity or to the NTD. The very high accuracy of the NTD (<20 ps) provides a good measure of the bang time uncertainty of the NBT system. Figure 88.7 shows the cross-calibration of the back channel of NBT and NTD using many targets shots with D_2-filled plastic capsules. A very good correlation between the NTD and back-channel NBT data is observed, with a spread of σ_{back} = 50 ps. A correlation of similar quality is found between the front and back channels of the NBT detector in the common range of sensitivity. Given the 650-ps rise time of the PMT, this is a very good agreement.

Because both NBT channels are analyzed by the same method, it is safe to assume that the bang time uncertainty from fitting the front-channel NBT data is the same as the measured back-channel spread: σ_{fit} = 50 ps. Adding the contributions from the x-ray calibration, σ_{calib}, σ_{dist}, and the uncertainty of

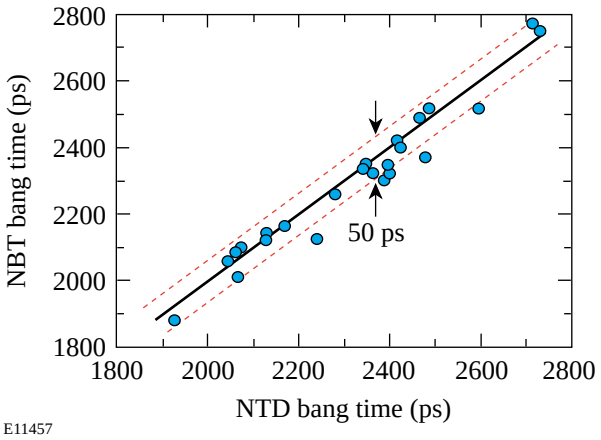

Figure 88.7
Cross-calibration between the back NBT channel and NTD. A very good correlation between NTD and NBT is observed with a rms difference of only 50 ps.

the bang time determination σ_{fit} in quadrature results in an overall absolute neutron bang time accuracy of $\sigma_{front} \leq 100$ ps for the x-ray-calibrated front NBT channel.

Summary and Conclusions

A simple, low-cost, two-channel neutron bang time detector having a wide dynamic range has been developed for OMEGA to complement the capabilities of the streak camera–based NTD. This instrument is able to measure the neutron bang time of D_2- and DT-filled capsules at a neutron yield between 10^7 and 10^{11} with an absolute timing accuracy of better than 100 ps, using hard x rays to calibrate the system. A high-stability fiducial system and a high-bandwidth, fast digitizing oscilloscope are both essential to achieve this precision. Neutron bang time uncertainty as low as 50 ps has been demonstrated using cross-calibrations to a higher-precision instrument such as the NTD. This level of accuracy allows the modeling of the implosions to be effectively guided using hydrocode calculations.

ACKNOWLEDGMENT

This work was supported by the U.S. Department of Energy Office of Inertial Confinement Fusion under Cooperative Agreement No. DE-FC03-92SF19460 and the University of Rochester. The support of DOE does not constitute an endorsement by DOE of the views expressed in this article.

REFERENCES

1. J. Nuckolls *et al.*, Nature **239**, 139 (1972).
2. N. Miyanaga *et al.*, Rev. Sci. Instrum. **61**, 3592 (1990).
3. T. J. Murphy and R. A. Lerche, *ICF Quarterly Report* **3**, 35, Lawrence Livermore National Laboratory, Livermore, CA, UCRL-LR-105821-93-1 (1992).
4. R. A. Lerche, D. W. Phillion, and G. L. Tietbohl, in *Ultrahigh- and High-Speed Photography, Videography, and Photonics '93*, edited by P. W. Roehrenbeck (SPIE, Bellingham, WA, 1993), Vol. 2002, pp. 153–161.
5. R. A. Lerche, D. W. Phillion, and G. L. Tietbohl, Rev. Sci. Instrum. **66**, 933 (1995).
6. Bicron Newbury, Newbury, OH 44065-9577.
7. Hamamatsu Photonics K.K. (http://www.hamamatsu.com).
8. Picosecond Pulse Labs, Boulder, CO 80301.
9. V. Yu. Glebov, D. D. Meyerhofer, C. Stoeckl, and J. D. Zuegel, Rev. Sci. Instrum. **72**, 824 (2001).
10. Tektronix Corporation, Beaverton, OR 97077.
11. Laboratory for Laser Energetics LLE Review **87**, 109, NTIS document No. DOE/SF/19460-397 (2001). Copies may be obtained from the National Technical Information Service, Springfield, VA 22161.
12. T. J. Murphy, R. E. Chrien, and K. A. Klare, Rev. Sci. Instrum. **68**, 610 (1997).